

## INSTRUMENTATION INTERFERENCE IN A TRANSONIC LINEAR CASCADE

G. Lopes, L. Simonassi, A.F.M. Torre, S. Lavagnoli  
*Turbomachinery and Propulsion Department  
von Karman Institute for Fluid Dynamics  
Sint-Genesius-Rode, Belgium  
[gustavo.lopes@vki.ac.be](mailto:gustavo.lopes@vki.ac.be)*

### ABSTRACT

A major challenge when testing high-speed flows in turbomachinery applications concerns instrumentation intrusiveness.

The current work exposes the impact of aerodynamic probes, placed upstream and downstream of the testing article, on the aerodynamics of a transonic low-pressure turbine blade investigated in a linear cascade at engine-representative outlet Mach and Reynolds numbers.

The effect of a probe placed downstream of the cascade can be perceived as far as to the inlet of the cascade. The quantification of the probe impact is presented on the blade loading as well as on the instrumentation placed upstream and downstream of the cascade used to monitor the operating conditions during testing.

It is shown that the presence of the probe can be partially compensated. The impact of this aerodynamic compensation on the cascade loss is reported.

### NOMENCLATURE

#### Abbreviations

|       |                                     |
|-------|-------------------------------------|
| CFD   | Computational Fluid Dynamics        |
| $g$   | Cascade pitch                       |
| GTF   | Geared Turbofan                     |
| LPT   | Low-pressure turbine                |
| $M$   | Mach number                         |
| out   | outlet                              |
| $Re$  | Reynolds number based on true chord |
| $S$   | Location along suction side         |
| $S_L$ | SS surface length                   |
| SS    | Suction side                        |
| $y$   | Pitchwise location                  |

#### Subscripts and superscripts

|         |                    |
|---------|--------------------|
| 1, 2, 6 | Measurement Planes |
| $is$    | Isentropic         |
| $MS$    | Midspan            |

### INTRODUCTION

The need to characterize flow interactions in high-speed low-pressure turbines (LPT) typically encountered in geared turbofans (GTF) requires high-fidelity experimental data at engine-representative conditions. High-speed turbomachinery rigs are often characterized by complex 3-D geometries and constrained accessibility to the test section which can be limiting for optical setups.

Multi-hole probes for which the stem is perpendicular to the flow being surveyed are still one of the most cost-effective and space-saving solutions to map the aerothermodynamic flow field in turbomachinery rigs. In

addition, they arguably remain the only reliable way to measure pressure losses.

However, the investigation of the flow physics by means of finite size instrumentation introduces non-negligible effects in the flow topology of the testing article [1] and the flow field itself. The latter is a combined effect of the interaction of the probe with the cascade potential field [2] and local blockage [3]. The impact of the probe becomes more severe as the flowfield Mach number ( $M$ ) approaches transonic values [4].

Truckenmuller and Stetter [1] investigated the interactions between multi-hole probes on the aerodynamics of a single-stage steam LPT. They found a strong influence of the probe on the flowfield and blade aerodynamics for a stem perpendicular to the incoming flow. The blockage effect promoted a decrease in dynamic pressure up to 15% compared to the undisturbed case.

Aschenbruck et al. [2] numerically and experimentally characterized the impact of a multi-hole probe on the flowfield between blade rows of a turbine operating at subsonic Mach number. They found and attributed differences between the CFD and experiments to the potential effect of the probe.

Sanders et al. [5] concluded that the impact of a probe measuring downstream of a transonic compressor can be perceived upstream of the blade passages in their numerical investigation.

Boerner et al. [4] highlighted the complexity of using multi-hole probes to characterize the aerodynamics of an LPT profile operating at transonic outlet Mach numbers in a linear cascade environment. They noticed a modification of the pressure field induced by the presence of a needle probe. They also report a reduction of the isentropic Mach number on the rear part of the blade suction side (SS) that is dependent on the probe location in relation to the measuring blade. The latter was attributed to probe blockage effects.

Torre et al. [6] have numerically assessed the impact of an L-shaped 5-hole probe on the aerodynamics of a transonic vane row. They have shown that the stagnation region in front of the probe generates a local reduction of the isentropic Mach number on the SS of the upstream vane, while low-pressure regions around the probe cause an increase of the isentropic Mach number on the SS of the adjacent vanes.

Current strategies to reduce the probe intrusiveness consist of miniaturizing the probe head size [7, 8] and having the probe measurement location as far from the stem as possible. The reduction of the head size is translated into a thinning of the line-cavity system diameter and a consequent significant reduction in response time [7].

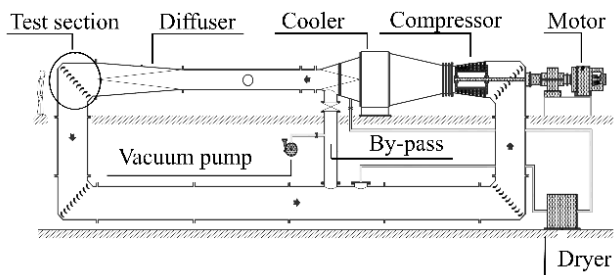


**Figure 1** Schematic of the VKI S1-C wind tunnel

This solution is therefore prohibiting in short duration facilities. Additionally, further miniaturization of probe geometries requires the use of advanced manufacturing techniques that may not be available to all research groups. Boerner and Niehuis [9] miniaturized an existing wedge probe for transonic flow measurements using Direct Metal Laser Sintering. On the other hand, increasing the distance between the head and stem is constrained by the available space between adjacent blade rows or the access points on existing facilities.

For the reasons depicted above, a quantification of the impact of existing probes on the aerodynamics of the testing article is necessary. In addition, strategies to mitigate and/or compensate the probe intrusiveness should be implemented.

## EXPERIMENTAL APPARATUS

### The VKI S-1/C

The measurements are conducted in the high-speed, low-Reynolds linear cascade S-1/C of the von Karman Institute. A schematic view of the wind tunnel is shown in Figure 1. The wind tunnel is a continuous closed-loop facility driven by a 615 kW 13 stages axial flow compressor. The flow temperature is kept near ambient by means of an air-to-water heat exchanger. The mass flow is regulated via the adjustment of the compressor rotational speed and a by-pass valve. A vacuum pump regulates the pressure level inside the facility, allowing to reach minimum absolute pressure values in the order of 5000 Pa. The cascade test section is mounted in the first elbow of the loop, following the diffuser. Wire meshes and honeycombs upstream of the test section ensure homogeneous inlet flow conditions. The outlet Mach and Reynolds numbers can be set independently, hence allowing to test a wide range of engine-relevant conditions. The freestream turbulence intensity (FSTI) can be imposed by means of a movable passive turbulence grid. Lastly, to recreate the effects of incoming unsteady wakes the facility can feature a spoked-wheel type wake generator (WG). The test section underwent a major refurbishment to enable the test of quasi 3-D flows with the presence of incoming wakes and purge flows [10]. More in-depth descriptions of the facility are reported in Arts et al. [11] and Clinkemaelle et al. [12].

### High-Speed Low-Pressure Turbine Cascade

The instrumentation interference has been investigated in the open-access SPLEEN C1 geometry. The geometry

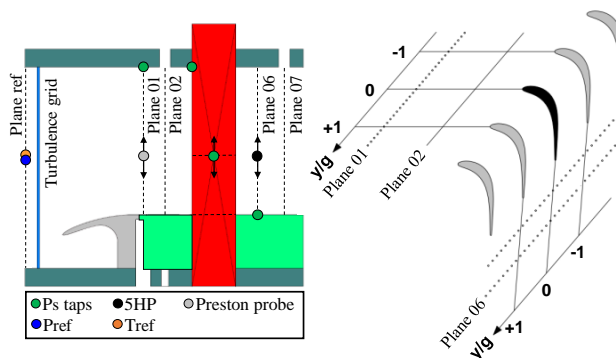


**Figure 2** Test section layout and instrumentation at each measurement plane and blade (left) and cross-sectional view of cascade pitchwise reference system (right)

and aerodynamic properties of the profile are discussed by Simonassi et al. [10]. The cascade consists of 23 blades with a span of 165 mm. The investigation is conducted for the nominal operating point ( $M_{6, is} = 0.900$ ;  $Re_{6, is} = 70k$ ) in the absence of unsteady incoming wakes. The freestream turbulence intensity is kept fixed at  $\sim 2.40\%$  by means of a passive turbulence grid.

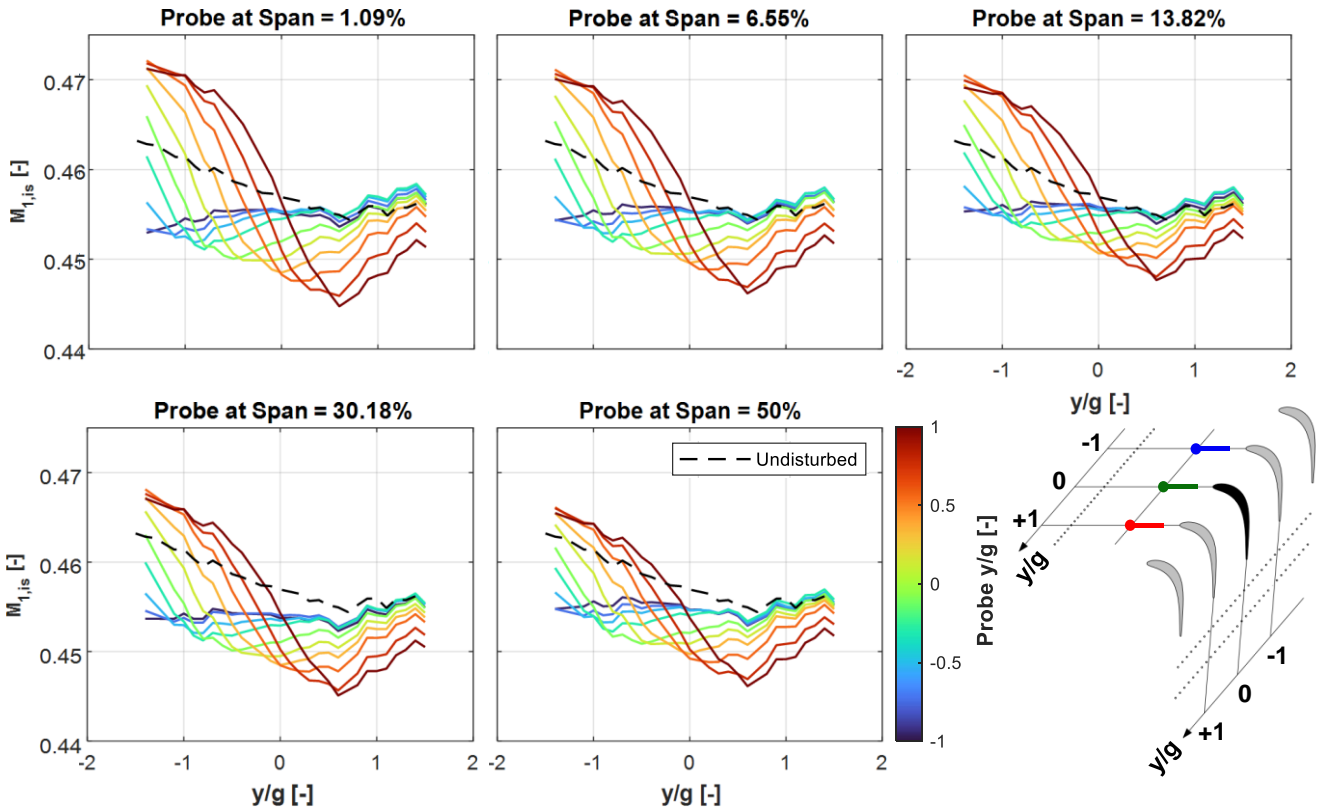
## Experimental Methodology

Figure 2 shows the meridional (left) and blade-to-blade (right) views of the test section, along with the measurement planes for reference.

The characterization of the probe intrusiveness is performed by means of pressure taps on the upper endwall at Plane 01, lower endwall at Plane 06 and blade suction side (SS). Plane 01 is instrumented with 31 taps with a diameter of 1.00 mm equally spaced along two pitches and connected to a Scanivalve MPS4264 – 1 PSI. Plane 06 is instrumented with 31 taps with a diameter of 1.00 mm equally spaced along four pitches and connected to a Scanivalve MPS4264 – 2.5 PSI. Both scanners are referenced to the total pressure at Plane Ref measured with a WIKA P-30 absolute pressure sensor with uncertainty of  $\pm 25$  Pa.

The isentropic Mach number computed at Plane 01 and Plane 06 is estimated with a propagated uncertainty of  $\pm 0.014$  (20:1) and  $\pm 0.010$  (20:1), respectively. The blade is instrumented with 24 SS taps with variable diameter and are connected to the same scanner as Plane 01 and the isentropic Mach number for these taps is computed with an uncertainty of  $\pm 0.010$  (20:1). More details on the instrumented blade can be found in [10].

The impact on the Plane 01 and 06 taps is investigated for the case of a Cobra 5-hole (5H) probe inserted and measuring at Plane 02. The same is performed for an L-shaped 5H probe inserted in Plane 07 which head measures at Plane 06. The geometry of both probes is displayed in Figure 4. In addition, the impact of the latter is investigated on the blade SS taps at 10%, 30% and 50% span by traversing the blade taps location. The location of both probes is varied along the span and pitchwise directions.



**Figure 3** Impact of Cobra 5-hole probe on pitchwise distribution of isentropic Mach number Plane 01 taps. Each plot represents a fixed spanwise location of the probe. The colormap denotes the pitchwise location of the probe

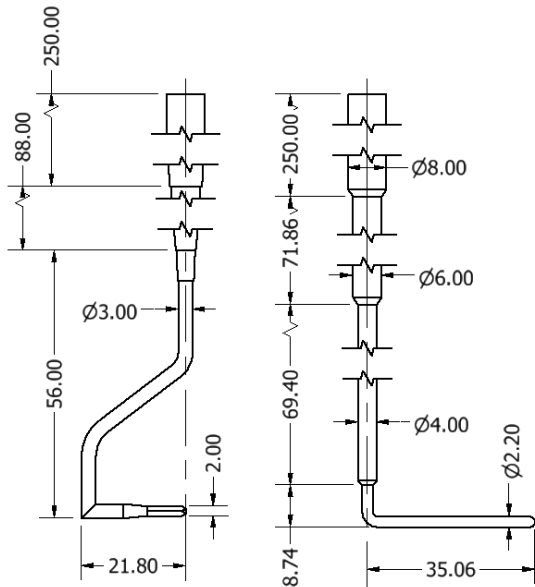


**Figure 4** Geometry of (left) Cobra 5-hole measuring at Plane 02 and (right) L-shaped 5-hole probe measuring at Plane 06

## RESULTS

### Influence of Cobra 5H Probe on Plane 01

Figure 3 displays the impact of traversing the Cobra 5H probe at the cascade inlet on the isentropic Mach number ( $M_{is}$ ) computed with the pressure taps at Plane 01. Each figure contains the distributions as the probe traverses along the pitch for a fixed spanwise location. The colormap represents the probe pitchwise location. The undisturbed distribution is represented with a dashed black line. The greatest impact on the isentropic Mach number distribution

occurs when the probe sits at  $y/g = +1.00$ , regardless of the spanwise location. The increased value of  $M_{is}$  measured at Plane 01 when the probe is at this location suggests a redistribution of the massflow towards the passage above the central blade due to the probe blockage. The latter effect is supported by the reduction of  $M_{is}$  in the passage obstructed by the probe and agrees with the numerical study of Sanders *et al.* [5]. For a fixed spanwise location, it is found that the probe blockage has decreasingly impact for decreasing values of  $y_{probe}/g$ . When the probe is at  $y_{probe}/g = -1.09$  the maximum pitch-to-pitch variation of  $M_{is}$  amounts to  $\pm 0.001$ . It is concluded that the probe has an impact on passages above the probe location ( $y/g(y/g) > y_{probe}/g$ ).

As the spanwise location of the probe increases, and probe immersion decreases, a reduction in the overshoot of  $M_{is}$  at  $y_{tap}/g = -1.50$  by 0.004 is visible. A reduction in the undershoot of  $M_{is}$  at  $y_{tap}/g = +0.80$  by 0.003 is also observed. When the probe is at the lowest pitchwise position, the reduction in probe immersion does not translate into significant variations in the  $M_{is}$  distribution. However, the undisturbed distribution is never fully recovered in the presence of the probe.

### Influence of L-Shape 5H Probe on Upstream Plane

The considerations drawn on the redistribution of massflow are further investigated by assessing the impact of a downstream mounted probe on the inlet flow to the cascade. Figure 5 displays the impact of traversing the L-shaped 5H probe at the cascade outlet on the isentropic Mach number computed with the pressure taps at Plane 01.

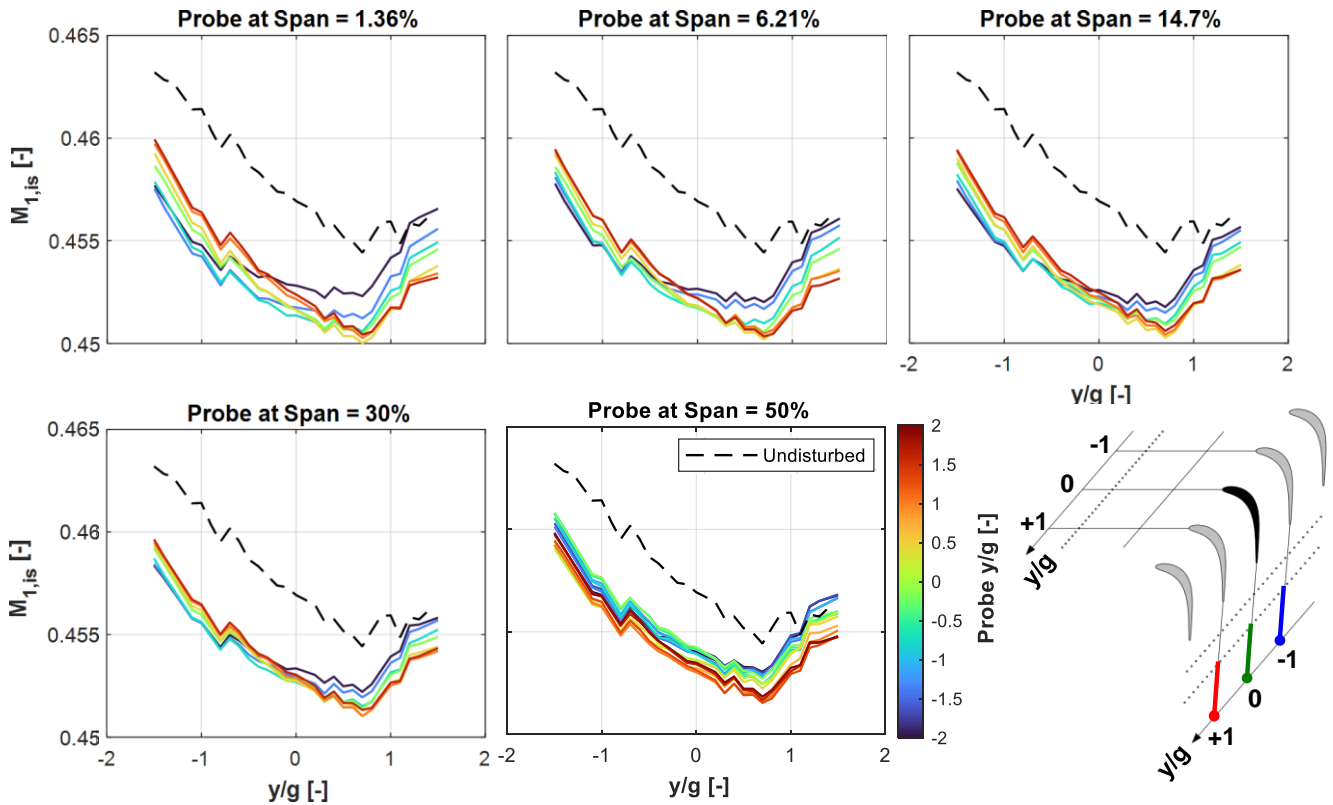


**Figure 5** Impact of L-shaped 5H probe on pitchwise distribution of isentropic Mach number Plane 06 taps. Each plot represents a fixed spanwise location of the probe. The colormap denotes the pitchwise location of the probe

Each figure contains the distributions as the probe traverses along the pitch for a fixed spanwise location. The colormap represents the probe pitchwise location.

The overall impact induced by the probe blockage is decreased as the probe immersion in the flow decreases. This is perceptible in the reduction of the maximum variation in the  $M_{is}$  measured at  $y_{tap}/g = +1.50$  from  $\pm 0.002$  to  $\pm 0.001$ . For all spanwise locations, the probe impact is greater for  $y/g > -0.5$ .

The impact of the probe on redistribution the massflow is also observed when the probe stem is at Plane 07. The presence of the probe promotes a reduction of the  $M_{is}$  in the taps within the cascade passage being blocked. This is visible as a crossing of the isentropic Mach number distributions depending on the probe location. The effect is more evident when the probe is measuring below 30% span. Figure 5 also allows to conclude that the isentropic Mach number at Plane 01 is never fully recoverable in the presence of the probe downstream. As it will be detailed later in this work, the nominal passage massflow is never fully recovered when probes are immersed in the flow unless a compensation is applied.

#### Influence of L-Shaped 5H Probe in Plane 06

Figure 6 displays the impact of traversing the L-shaped 5H probe at the cascade outlet on the isentropic Mach number computed with the pressure taps at Plane 06. Each figure contains the distributions as the probe traverses along the pitch for a fixed spanwise location. The colormap represents the probe pitchwise location.

The impact of the probe on the tap readings is significant when the probe is located near the endwall. This

can be seen a local under/overshoots in the Mach number distribution resultant from the distance from the probe head to the endwall that is smaller than the one suggested in [13] to neglect wall proximity effects. In fact, when the probe head is at 1.21% span, the under/overshoots are caused due to a local acceleration of the flow between the probe head and the pressure taps at similar  $y/g$ . This wall proximity effect causes fluctuations in the Mach number as large as  $\pm 0.073$ . This is confirmed by the significant reduction in the over/undershoot around  $M_{is} \approx 0.85$  as the spanwise location of the probe head increases from 1.21% to 3.84%.

An additional effect concerning the overall probe blockage is observed by the large increase of the Mach number above unity when the probe immersion is maximum. This effect results from the redistribution of massflow that is reported in the previous sections. Even though the probe is aligned with the outlet metal angle, the variations of angle in the secondary flow region and even the underturning that often occurs at midspan in LPTs increases the probe “frontal” area accountable for the blockage above its minimum value.

Up to 6.21% span, the probe blockage can cause an increase of the isentropic Mach number in the adjacent lower passage above unity. As the probe shifts towards positive  $y_{probe}/g$ , the impacted region also shifts. The region where  $y/g < y_{probe}/g$  displays minor impact. Even though not as severe, the behavior of the isentropic Mach number as the probe is translated is observed up to 50% span. For the case when the probe is at 50% span, an increase in the Mach number up to  $\approx 0.004$  is still existent

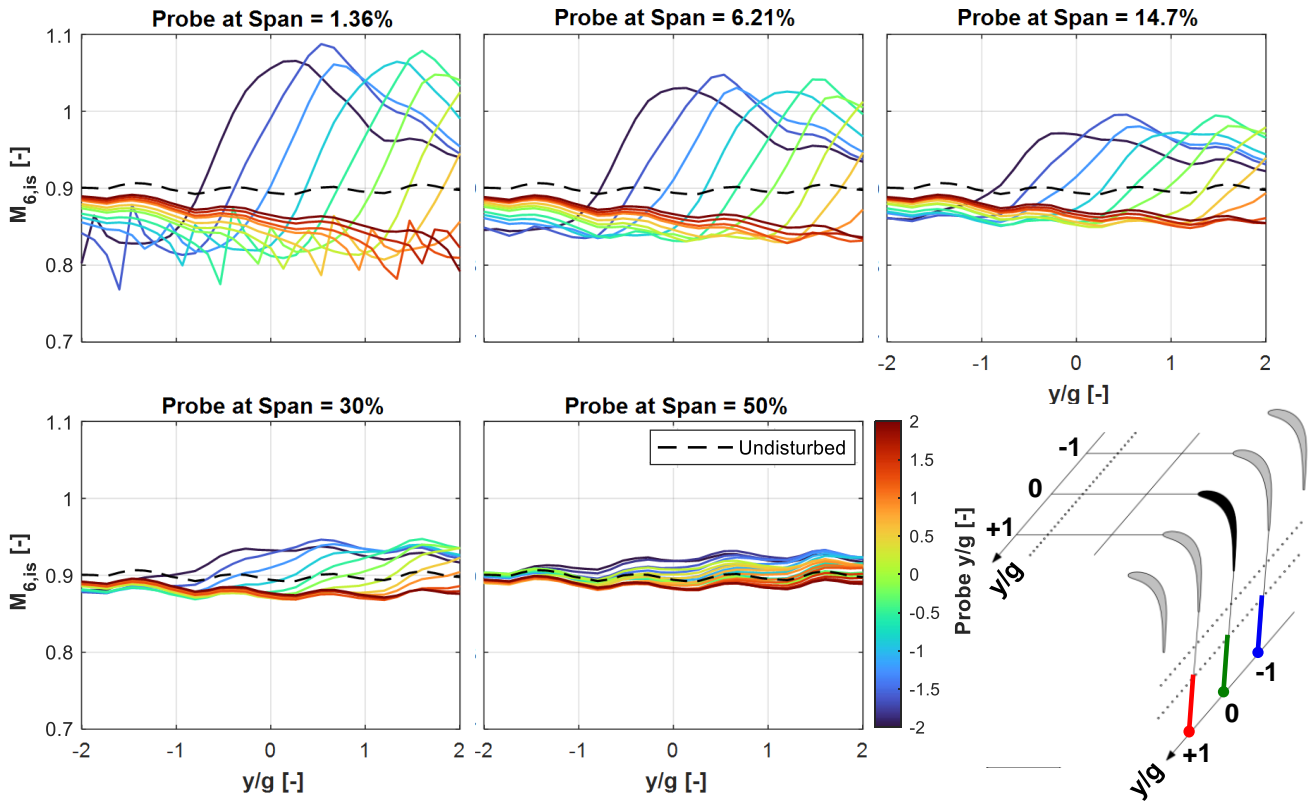


**Figure 6** Impact of L-shaped 5H probe on pitchwise distribution of isentropic Mach number Plane 01 taps. Each plot represents a fixed spanwise location of the probe. The colormap denotes the pitchwise location of the probe

on the passages where  $y/g > y_{probe}/g$ . The effect on the passages above becomes decreasingly small as the probe reaches  $y_{probe}/g = +2.00$ .

Once again, this behavior suggests that the passage below the probe is supplied with additional massflow induced by probe blockage. Even though this effect is greatly reduced when the probe is at 50% span and  $y_{probe}/g = +2.00$ , the undisturbed distribution is never fully recovered due to the probe.

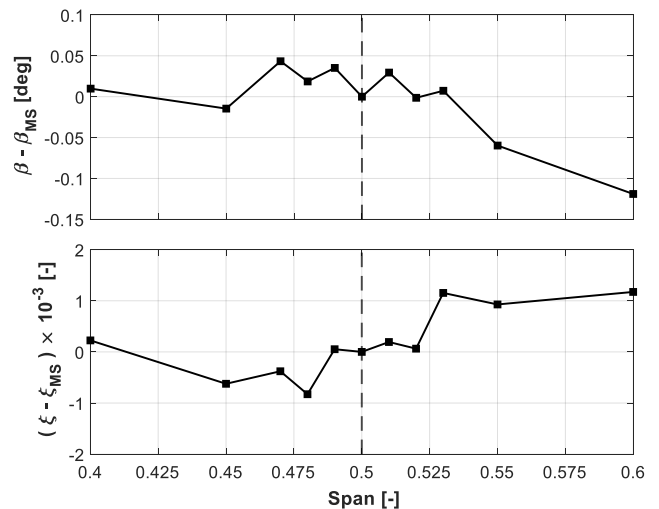
#### Influence of Blade Taps on Downstream Flow

Even though the blade SS taps' geometry and dimension are expected to have negligible interference on the flow field itself [12:14], an experimental validation is performed. Figure 7 contains the spanwise distribution of the area-averaged outlet flow angle (top) and mass-averaged energy loss coefficient (bottom) measured at Plane 06. The results are presented as the deviation from the midspan value where the SS blade taps are placed.

As displayed, the angle variation remains within  $\pm 0.10^\circ$  from 40% span to 60% span. However, if a region near the taps is assessed (45% to 55% span) the variation limits are further reduced to  $\pm 0.05^\circ$ . On the other hand, the energy loss coefficient is bounded between  $\pm 0.001$ , hence allowing to conclude that the blade SS taps have negligible impact on the downstream flow field.

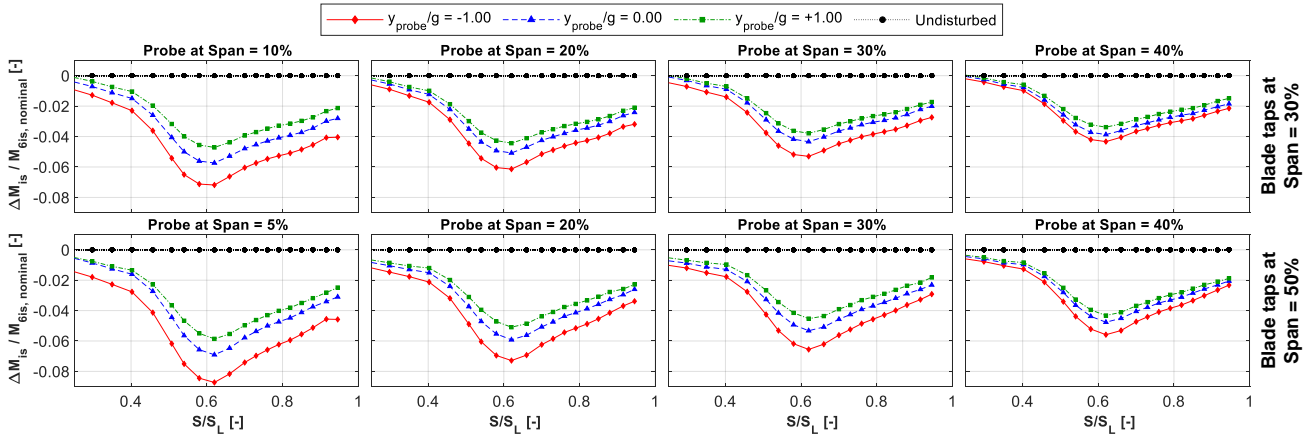
#### Influence of L-Shaped 5H Probe in Blade Aerodynamics

Figure 8 displays the deviation in the  $M_{is}$  distribution computed as  $\Delta M_{is} = M_{is,disturbed} - M_{is,undisturbed}$



**Figure 7** Impact of blade SS taps on outlet area-averaged flow angle (top) and mass-averaged energy loss coefficient (bottom) at Plane 06. Blade taps sit at 50% span

measured on the blade SS for different spanwise and pitchwise locations of the L-shaped 5H probe. The value is normalized by the nominal  $M_{out,is}$  ( $= 0.900$ ). Therefore, a negative  $\Delta M_{is}$  denotes a lower local value than for the undisturbed case. Like the previous sections, each sub-figure represents the case where the probe is at a fixed spanwise location and is traversed across the cascade pitch. The upper and lower rows contain the  $M_{is}$  distributions when the blade taps are at 30% and 50% span, respectively.



**Figure 8** Impact of L-shaped 5H probe on SS surface isentropic Mach number. Plots for disturbed case are normalized by the isentropic Mach number distribution of undisturbed case. Each plot represents a fixed spanwise location of the probe. First row displays case when blade taps sit at 30% span and bottom row displays case when blade taps sit at 50% span

For the same operating point of the linear cascade, the presence of the probe is translated into a reduction of the Mach number on the SS regardless of the probe location. For a fixed pitchwise location, it can be observed that the distribution is partially recovered as the probe immersion is reduced for both when the taps are at 30% span or 50% span. For any spanwise location of the probe, the highest impact on the Mach number distribution occurs when the probe is above the central blade ( $y/g < 0$ ). As detailed before, the underturning encountered at the cascade outlet promotes an increase of the probe effective frontal area which leads to a higher blockage of the passage that includes the blade SS instrumentation and therefore to the reduction of the isentropic Mach number on the SS. This effect decreases as  $y_{probe}/g$  increases. This effect has been observed experimentally by Boerner et al. [4] and numerically by Torre et al. [6] in transonic cascade setups. Lastly, for a fixed span and pitchwise locations of the probe, a higher impact of the probe blockage on the Mach number distribution is noticed when the blade taps sit at 50% span. A maximum deficit in the local isentropic Mach number from the undisturbed case of  $\approx 0.085$  at  $S/S_L = 0.62$  is found when the probe sits at 5% span and  $y_{probe}/g = -1.00$ , and the blade taps are measuring at 50% span. The minimum deficit at  $S/S_L = 0.62$  amounts to  $\approx 0.034$  when the probe sits at 40% span and  $y/g = +1.00$ , and the blade taps are measuring at 30% span.

### Compensation of Probe Interference

Since the probe reduces the massflow through the cascade passage under investigation, the blade and flowfield aerodynamics under investigation are altered from the nominal operating point. To compensate for the probe blockage, the massflow through the cascade test section is increased to retrieve the nominal operating point.

Figure 9 displays the deviation in the  $M_{is}$  distribution computed as  $\Delta M_{is} = M_{is,disturbed} - M_{is,undisturbed}$  and normalized by the nominal outlet Mach number measured on the blade SS. Each sub-figure contains the  $\Delta M_{is}$  distribution for a fixed probe location, with the different lines represent increasing outlet Mach numbers obtained by increasing the overall mass flow through the cascade.

Regardless of the outlet Mach number, similar probe impact as described before is observed. For a fixed  $y_{probe}/g$  and blade taps spanwise location, the isentropic Mach number measured on the blade surface increases as the probe immersion is reduced (left to right columns in Figure 9). Similarly, there is an increase in the blade SS isentropic Mach number as  $y_{probe}/g$  increases for a fixed probe and blade taps spanwise location.

The main difference with respect to the probe impact on the blade for a fixed outlet Mach number is that for a fixed spanwise and pitchwise locations of the probe, an increase of the outlet Mach number enables retrieving the nominal blade loading without a probe immersed in the flow. Consequently, for reduced probe intrusiveness locations, the blade loading is higher than the nominal one.

Since the difference between the non-disturbed and the disturbed blade loadings is a function of the probe immersion, probe pitchwise location and outlet Mach number, a compromise must be achieved to guarantee that the compensation for the probe interference does not produce unrealistic aerodynamics on the blade SS and downstream flow field. Simonassi et al. [10] show the high pitch-to-pitch periodicity in the VKI S-1/C cascade. Therefore, the characterization of the blade and cascade aerodynamics can be restricted to a single blade.

By surveying the flow field between  $y/g=0.00$  and  $+1.00$ , and between the endwall and 50% span, the maximum  $\Delta M_{is}$  from the undisturbed case can be constrained between  $\Delta M_{is} = \pm 0.015$ ,  $\pm 0.024$  and  $\pm 0.025$  when the blade taps are at 10%, 30% and 50%, respectively. Since the maximum variation occurs near the velocity peak, the deviation in the isentropic Mach number near the TE is half than the one at  $S/S_L \approx 0.60$ .

If no compensation is applied, the deficit of the isentropic Mach number compared to the undisturbed case can be as high as  $\pm 0.051$ ,  $\pm 0.059$  and  $\pm 0.062$  when the blade taps are at 10%, 30% and 50%, respectively.

From the blade analysis, the operating point respective to  $M_{6,is}=0.92$  is regarded as the one that allows to test near the nominal operating point in the absence of a downstream mounted probe.

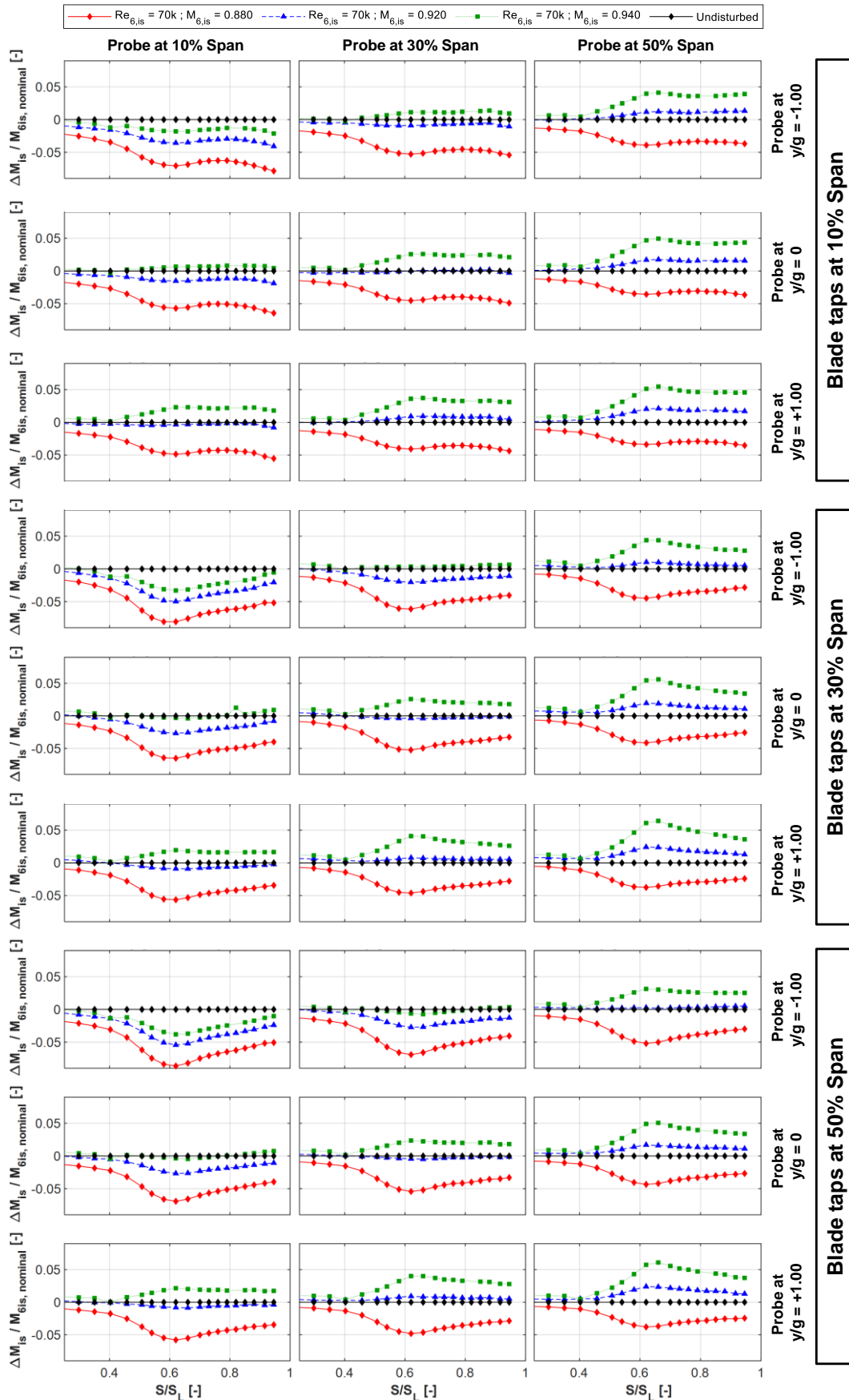


**Figure 9** Impact of compensating the  $M_{is}$  deficit on the blade SS by varying the cascade operating point when the probe is at different pitchwise and spanwise locations. First, second, third and fourth columns represent situations where the probe sits at 10%, 30%, 50% and 60% span, respectively.

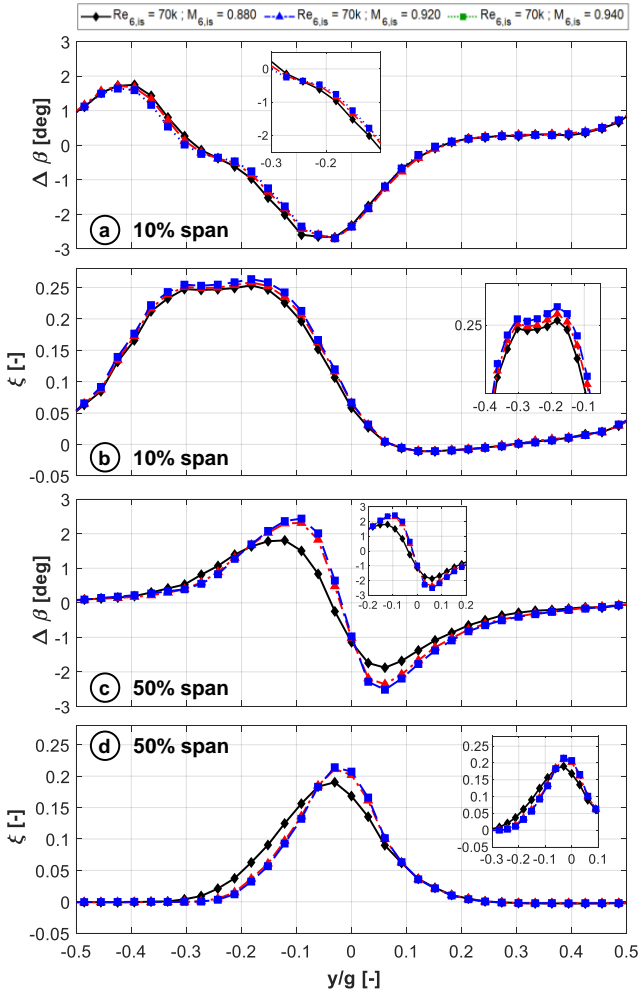


**Figure 10** Impact of compensating the  $M_{is}$  deficit on the pitchwise distribution of (a,c) deviation in primary flow direction and (b,d) energy loss coefficient at 10% span and 50% span, respectively.

Figure 10 displays the pitchwise distribution of the variation in primary flow direction at 10% span (a) and 50% span (b) as a function of the achieved outlet Mach number. In addition, the pitchwise distributions of the energy loss coefficient at 10% span (c) and 50% span (d) are also displayed. The computation of the energy loss coefficient is the described in [17]. At 10% span, the modification of the outlet Mach number mainly modifies the primary flow direction and losses associated with secondary flows present at this location. The highest impact occurs for  $y/g$  between  $-0.30$  and  $-0.10$ . In this region, the maximum variation in the  $\beta$  is within  $\pm 0.122^\circ$ . On the other hand, the maximum variation in the  $\xi$  is within  $0.01$  in a region where the loss amounts to  $\approx 0.25$ . At 50% span, the most impacted region sits between  $y/g = -0.20$  and  $+0.20$ . For the lowest Mach number investigated there is a thickening of the wake, reinforcing the need to compensate for probe interference. In this region, deviations from the primary flow direction as big as  $1.00^\circ$  are present. In the center of the wake, the deviation in the energy loss coefficient that amounts to  $0.024$ . The latter amounts for around 10% of the local energy loss coefficient. If the case of  $M_{6,is} = 0.88$ , for which the wake is modified, is removed from the analysis the deviation in  $\beta$  and  $\xi$  are reduced to  $0.19^\circ$  and  $0.005$ ,

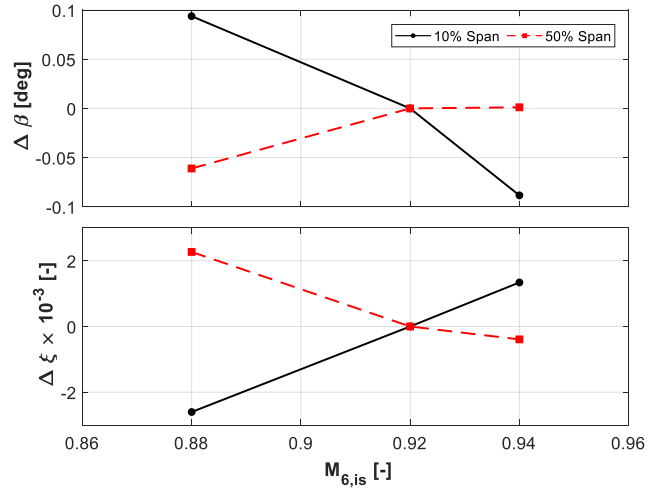


**Figure 11** Impact of compensating the  $M_{is}$  deficit on the (top) area-averaged primary flow direction and (bottom) mass-averaged energy loss coefficient.

respectively. It is worth mentioning that if no compensation is applied, the probe is measuring the flow field relative to the case of lowest Mach number for which there is a change of the wake topology.

Figure 11 displays the area-averaged primary flow direction (top) and mass-averaged energy loss coefficient (bottom), respectively. The quantities are plotted as deviation to the compensated operating point ( $M_{6,is} = 0.92$ ). The probe compensation introduces negligible variations in both quantities. The maximum variation in the area-averaged primary flow direction (Figure 11 – top) is within  $\pm 0.10^\circ$  at 10% span and it monotonically decreases with the outlet Mach number. On the other hand, the maximum variation at 50% span is within  $\pm 0.05^\circ$  and does not vary as the outlet Mach number increases from  $\pm 0.10^\circ$  to  $M_{6,is} = 0.94$ . The energy loss coefficient (Figure 11 – bottom) increases monotonically as the  $\pm 0.10^\circ$  increases and the probe measures at 10% span. Nonetheless, the maximum deviation is within  $\pm 0.10^\circ$ . The opposite is observed at 50% span, as the energy loss coefficient monotonically decreases. These findings are supported by the work of Torre et al. [6].

### Monitoring of Rig Operating Point

Due to the impact of the L-shaped 5H probe on the static pressure at Plane 06, the flow conditions that are typically set based on these taps do not represent the operating point of the cascade. To estimate and track the flow conditions in the test section, static pressure measurements in a region not impacted by the probe are used. In the VKI S-1/C cascade, a base pressure tap downstream of the cascade (see Figure 12) and upstream of a wire mesh is used to compute the isentropic Mach number using the freestream total pressure. A calibration of the isentropic Mach number in the base pressure region against the one measured at Plane 06 in the absence of the probe can be obtained and used to track the operating point when the probe is installed.

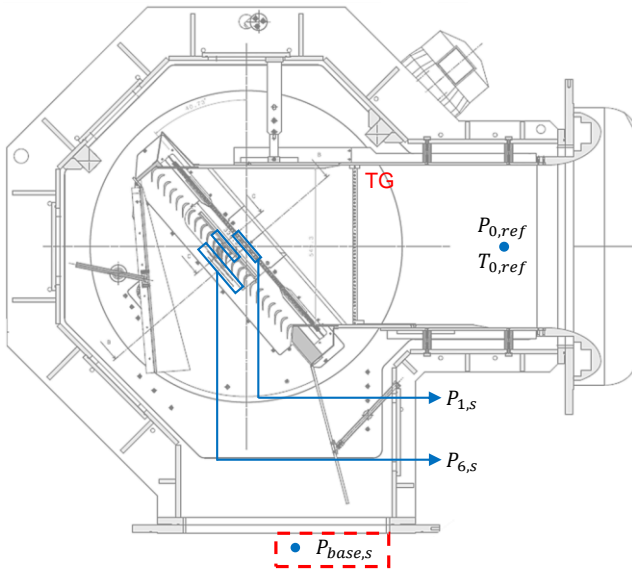


**Figure 12** VKI S-1/C linear cascade and location of measurement planes including base pressure location

Figure 12 displays the evolution in the isentropic Mach number during a traverse performed at Plane 06 with the L-shaped 5H probe for  $M_{6,is} \approx 0.920$ . The spanwise location of the probe increases with the acquisition number. The solid black line denotes the isentropic Mach number measured at the base region. The colored lines denote the isentropic Mach number obtained by averaging the measurements from the Plane 06 static taps. The different colors represent a different number of taps used to average the Mach number. The increase in taps used for the average follows the pitchwise reference system of the cascade (i.e. seven taps means that the first seven taps starting from the most negative  $y/g$  are used). As the number of taps used for averaging is reduced, the oscillations induced by the probe decrease. However, the operating point Mach number is never retrieved. The Mach number converges to the nominal compensated one as the probe immersion in the test section is reduced. On the other hand, the isentropic Mach number computed at the base region displays a very stable behavior and therefore is suitable to track the rig operating point. The stability of the rig is demonstrated in [10]. Lastly, if the calibration described above is applied, one can estimate the Mach number in the test section as displayed by the dashed black line in Figure 13.

## CONCLUSIONS

- Impact of probe mounted downstream can be seen as far as  $0.50Cax$  upstream of LE. Interaction may occur if wake generator is present.
- Blade aerodynamics is greatly modified and therefore characterization should be performed in absence of probes in test section
- Probe impact modifies the pitchwise distribution of aerodynamic quantities at the endwall locations. However, the variation of the averaged quantities is reduced.
- Compensation of probe interference can be accounted by increase massflow rate in test section

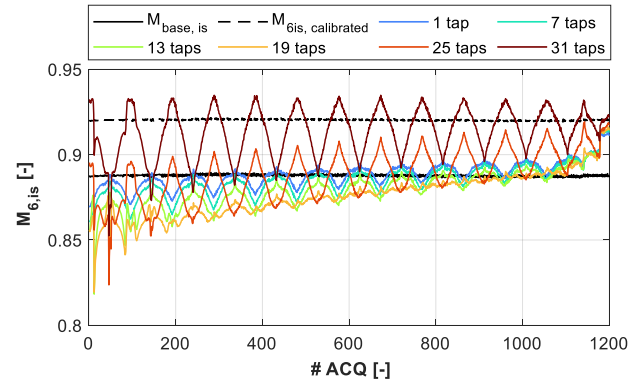


**Figure 13** Outlet isentropic Mach number evolution during traverse performed with L-shaped 5-hole probe at Plane 06.

## ACKNOWLEDGMENTS

The authors gratefully acknowledge funding of the SPLEEN project by the Clean Sky 2 Joint Undertaking under the European Union's Horizon 2020 research and innovation program under the grant agreement 820883.

## REFERENCES

- [1] F. Truckenmüller and H. Stetter, "Measurement errors with pneumatic probes behind guide vanes in transonic flow-fields," 1996.
- [2] J. Aschenbruck, T. Hauptmann, and J. R. Seume, "Influence of a multi-hole pressure probe on the flow field in axial-turbines," 2015.
- [3] J. S. Wyler, "Probe blockage effects in free jets and closed tunnels," 1975.
- [4] M. Boerner, M. Bitter, and R. Niehuis, "On the challenge of five-hole-probe measurements at high subsonic Mach numbers in the wake of transonic turbine cascades," *Journal of the Global Power and Propulsion Society*, vol. 2, pp. 453–464, 2018.
- [5] C. Sanders, M. Terstegen, M. Hölle, P. Jeschke, H. Schönenborn, and T. Fröbel, "Numerical studies on the intrusive influence of a five-hole pressure probe in a high-speed axial compressor," in *Turbo Expo: Power for Land, Sea, and Air*, 2017, vol. 50787, p. V02AT39A009.
- [6] A. F. M. Torre, M. Patinios, G. Lopes, L. Simonassi, and S. Lavagnoli, "Vane-Probe Interactions in Transonic Flows," in *ASME Turbo Expo 2022: Turbine Technical Conference and Exposition (pp. GT2022-82549)*. The American Society of Mechanical Engineers (ASME), 2022.
- [7] S. D. Grimshaw and J. V. Taylor, "Fast settling millimetre-scale five-hole probes," in *Turbo Expo: Power for Land, Sea, and Air*, 2016, vol. 49828, p. V006T05A014.
- [8] J. Town and C. Camci, "Sub-miniature five-hole probe calibration using a time efficient pitch and yaw mechanism and accuracy improvements," in *Turbo Expo: Power for Land, Sea, and Air*, 2011, vol. 54631, pp. 349–359.
- [9] M. Boerner and R. Niehuis, "Development of an additive manufactured miniaturized wedge probe optimized for 2D transonic wake flow measurements," 2018.
- [10] L. Simonassi, G. Lopes, S. Gendebien, A. F. M. Torre, M. Patinios, and S. Lavagnoli, "An Experimental Test Case for Transonic Low-Pressure Turbines - Part 1: Rig Design, Instrumentation and Experimental Methodology," in *ASME Turbo Expo 2022: Turbine Technical Conference and Exposition (pp. GT2022-81566)*. The American Society of Mechanical Engineers (ASME).
- [11] T. Arts, "Aerodynamic performance of two very high lift low pressure turbine airfoils (T106C–T2) at low Reynolds and high Mach numbers," 2013.
- [12] J. Clinckemaillie, L. Fattorini, T. Fontani, C. Nuyts, G. Wain, and T. Arts, "Aerodynamic performance of a very-high-lift low-pressure turbine airfoil (T106C) at low Reynolds and high Mach number including the effect of incoming periodic wakes," 2015.
- [13] F. A. MacMillan, "Experiments on Pitot-tubes in shear flow," 1956.
- [14] R. Shaw, "The influence of hole dimensions on static pressure measurements," *Journal of fluid mechanics*, vol. 7, no. 4, pp. 550–564, 1960.
- [15] J. L. Livesey, J. D. Jackson, and C. J. Southern, "The Static Hole Error Problem: An Experimental Investigation of Errors for Holes of Varying Diameters and Depths," *Aircraft Engineering and Aerospace Technology*, 1962.
- [16] R. E. Rayle, "An investigation of the influence of orifice geometry on static pressure measurements," PhD Thesis, Massachusetts Institute of Technology, 1949.
- [17] G. Lopes, L. Simonassi, A. F. M. Torre, M. Patinios, and S. Lavagnoli, "An Experimental Test Case for Transonic Low-Pressure Turbines - Part 2: Cascade Aerodynamics at On- and Off- Design Reynolds and Mach Numbers," in *ASME Turbo Expo 2022: Turbine Technical Conference and Exposition (pp. GT2022-82626)*. The American Society of Mechanical Engineers (ASME).